Seed-Mediated Synthesis of Gold Nanorods: Role of the Size and Nature of the Seed

Anand Gole and Catherine J. Murphy*

Department of Chemistry and Biochemistry, University of South Carolina, Columbia, South Carolina 29208

Received May 14, 2004. Revised Manuscript Received July 14, 2004

We report studies on the synthesis of gold nanorods by a three-step seeding protocol method using a variety of different gold seeds. The synthetic method is adapted from one we published earlier (Jana et al. *J. Phys. Chem. B* **2001**, *105*, 4065). The seeds chosen for these studies have average diameters in the range from 4 to 18 nm, with positively charged as well as negatively charged surface groups. In all the cases, along with a large concentration of long rods, a small number of different shapes such as triangles, hexagons, and small rods are observed. The proportion of small rods increases with an increase in the seed size used for nanorod synthesis. For long nanorods synthesized by different seeds a comparison of various parameters such as length, width, and aspect ratio has been made. A dependence of the nanorod aspect ratio on the size of the seed is observed. Increasing the seed size results in lowering of the gold nanorod aspect ratios for a constant concentration of reagents. The charge on the seed also plays a role in determining the nanorod aspect ratio. For positively charged seeds variation in the aspect ratio is not as pronounced as that for negatively charged seeds. The gold nanorods synthesized were characterized by transmission electron microscopy (TEM), UV−vis spectroscopy, and Fourier transform infrared spectroscopy. The role of seed size in the size and shape evolution of the nanocrystal, at different growth stages, has been studied by TEM.

Introduction

The unusual physicochemical and optoelectronic properties of nanomaterials[1−3] hold tremendous potential in the synthesis and design of various advanced materials. These unusual properties depend on both individual and collective properties of nanoparticles and their sizes and shapes.[4−6] It is now well-known that variation in dimensionality is critical in determining the different electronic properties of nanomaterials.[7] There is a considerable current interest in 1-D semiconductor nanostructures (nanorods and nanotubes) due to their efficiency in electron-transport processes and utility in other electronic devices.[8] Metal nanorods and nanowires too have fundamentally interesting properties, such as strong surface-enhanced Raman scattering (SERS),[9] fluorescence,[10] and anisotropic chemical reactivity.[11] A variety of synthetic protocols are available for the synthesis of metal and semiconductor nanorods with different sizes and aspect ratios. Rigid templates such as membranes[12−14] have been used wherein metal/semiconductor ions are reduced/reacted inside their nanoscale pores. Metal carbide and nitride nanorods have been synthesized by reacting volatile transition-metal and main-group halide or oxide species with carbon nanotube templates.[15,16] This yields nanorods which have dimensions comparable to those of their templates, and hence, effectively a variety of sizes can be synthesized. Colloidal routes employing surfactants as directing agents using electrochemical[17] and seed-mediated growth methods for the synthesis of nanorods have also been developed.[18−23] Our group[18−22,25,28] is actively involved in fine-tuning the seed-mediated route for the colloidal synthesis of gold and silver nanorods.

* To whom correspondence should be addressed. E-mail: Murphy@mail.chem.sc.edu.

(1) Henglein, A. *Top. Curr. Chem.* **1988**, *143*, 113.
(2) Wang, Y.; Herron, N. *J. Phys. Chem.* **1991**, *95*, 525.
(3) Alivisatos, A. P. *Science* **1996**, *271*, 933.
(4) Link, S.; El-Sayed, M. A. *J. Phys. Chem. B* **1999**, *103*, 8410.
(5) Storhoff, J. J.; Lazarides, A. A.; Mirkin, C. A.; Letsinger, R. L.; Mucic, R. C.; Schatz, G. C. *J. Am. Chem. Soc.* **2000**, *122*, 4640.
(6) El-Sayed, M. *Acc. Chem. Res.* **1999**, *34*, 257.
(7) Lieber, C. M.; Wu, X. L. *Acc. Chem. Res.* **1991**, *24*, 223.
(8) Hu, J.; Odom, T. W.; Lieber, C. M. *Acc. Chem. Res.* **1999**, *32*, 435.
(9) Nikoobakht, B.; Wang, J.; El-Sayed, M. A. *Chem. Phys. Lett.* **2002**, *366*, 17.
(10) Mohamed, M. B.; Volkov, V.; Link, S.; El-Sayed, M. A. *Chem. Phys. Lett.* **2000**, *317*, 517.
(11) Jana, N. R.; Gearheart, L.; Obare, S. O.; Murphy, C. J. *Langmuir* **2002**, *18*, 922.
(12) Martin, C. R. *Chem. Mater.* **1996**, *8*, 1739.
(13) Martin, B. R.; Dermody, D. J.; Reiss, B. D.; Fang, M. L.; Lyon, A.; Natan, M. J.; Mallouk, T. E. *Adv. Mater.* **1999**, *11*, 1021.
(14) Wu, C.-G.; Bein, T. *Science* **1994**, *266*, 1013.
(15) Han, W. Q.; Fan, S. S.; Li, Q. Q.; Hu, Y. D. *Science* **1997**, *277*, 1287.
(16) Wong, E. W.; Benjamin, W. M.; Burns, L. D.; Lieber, C. M. *Chem. Mater.* **1996**, *8*, 2041.
(17) Ying, Y.; Chang, S. S.; Lee, C. L.; Wang, C. R. C. *J. Phys. Chem. B* **1997**, *101*, 6661.
(18) Jana, N. R.; Gearheart, L.; Murphy, C. J. *J. Phys. Chem. B* **2001**, *105*, 4065.
(19) Jana, N. R.; Gearheart, L.; Murphy, C. J. *Chem. Commun.* **2001**, 617.
(20) Caswell, K. K.; Bender, C. M.; Murphy, C. J. *Nano Lett.* **2003**, *3*, 667.
(21) Murphy, C. J.; Jana, N. R. *Adv. Mater.* **2002**, *14*, 80.
(22) Busbee, B. D.; Obare, S. O.; Murphy, C. J. *Adv. Mater.* **2003**, *15*, 414.
(23) Nikoobakht, B.; El-Sayed, M. A. *Chem. Mater.* **2003**, *15*, 1957.

10.1021/cm0492336 CCC: $27.50
Published on Web 08/28/2004

In this route, gold seeds, size range 3−4 nm, are first synthesized by chemical reduction of gold salt with a strong reducing agent (sodium borohydride) in the presence of a capping agent (citrate). These seeds are then added to a solution containing more metal salt, a weak reducing agent (e.g., ascorbic acid), and a surfactant-directing agent (cetyltrimethylammonium bromide, CTAB). These seeds serve as nucleation sites for the anisotropic growth of gold nanorods. This protocol gives fairly monodisperse, stable gold nanorods (stabilized by a bilayer of CTAB)[24] with different aspect ratios.[18,21]

To date, attempts have been made to understand the growth mechanism of nanorods using the seed-mediated protocols.[24−28] In our synthetic protocol, formation of pentatwinned nanostructures followed by preferential binding of the surfactant CTAB to a single-crystal face leads to the unidirectional growth of the crystal.[25] Recently we have reported the dependence of the gold nanorod aspect ratio on the nature of the surfactant used.[28] We found that the tail length of the surfactant is also important in controlling nanorod growth, presumably due to stabilization of the bilayer on the long faces of the nanorods.[28] In our ongoing effort to understand the role of different factors contributing to the evolution of the shape and size of the nanocrystals formed, we report herein the role of the seed on the gold nanorod synthesis. Different gold seeds in the size range from 4 to 18 nm with positively and negatively charged surface functionalities were used. It was found that the length, thickness, and aspect ratio of the gold nanorods depend on the size and nature of the seed used for the synthesis. The gold nanorods formed were characterized by UV−vis spectroscopy, Fourier transform infrared (FTIR) spectroscopy, and transmission electron microscopy (TEM) measurements. The different stages of nanorod synthesis such as the increase in size of the nanocrystals, generation of facets, and subsequent evolution into rods have been studied as a function of the seed size by TEM measurements.

Experimental Section

Materials. Chloroauric acid ($HAuCl_4 \cdot 3H_2O$), trisodium citrate, sodium borohydride ($NaBH_4$), ascorbic acid, and 4-mercaptobenzoic acid (4-MBA) were obtained from Aldrich and used as received. CTAB and D-glucose was obtained from Sigma and used without further purification. All the glassware was cleaned by aqua regia and rinsed with deionized water prior to the experiments.

Synthesis of Different Gold Nanoparticle Seeds. *Negatively Charged Nanoparticle Seeds. (a) A 3.5 nm Citrate-Stabilized Gold Seed.* The seeds were synthesized according to our method reported previously.[18] Typically this involves the preparation of a 20 mL aqueous solution containing 2.5×10^{-4} M $HAuCl_4$ and 2.5×10^{-4} M trisodium citrate. To this solution was added 0.6 mL of ice cold 0.1 M $NaBH_4$ with stirring. The solution immediately turned orange-red, indicating the formation of gold nanoparticles. The average particle size measured from transmission electron microscopy was 3.5 ± 0.7 nm.[18] Citrate serves as a capping agent in this case, and the gold particles are stable for a couple of weeks. The seed particles were stored at 25 °C for 3 h prior to any further experimentation, to allow excess borohydride to be decomposed by water.

(b) A 3.5 nm Uncapped Gold Seed. Gold seed particles were also prepared by the same method as used for the 3.5 nm citrate-stabilized seed, but now in the absence of sodium citrate. The average size of these seeds is 3.5 ± 0.7 nm as reported previously by Patil et al.[29] These uncapped gold seeds are also stable for a couple of weeks. These seed particles were stored at 25 °C for 3 h prior to any further experimentation.

(c) A 6.6 nm 4-MBA-Capped Gold Seed. A 10 mL sample of the citrate-stabilized seed solution (the 3.5 nm seed solution mentioned above in (a)), aged after 3 h of synthesis, was taken in a conical flask. Next, to this was added 250 μL of a 10^{-2} M ethanolic solution of 4-MBA with stirring. The color of the solution immediately turned dark red/purple, indicating surface modification of the gold nanoparticles by the thiol group of 4-MBA. The pH of the solution was ca. 8.0, and at this pH the carboxylic acid group of the 4-MBA is expected to be deprotonated and thus stabilize the gold nanoparticles against aggregation. The average particle size of these gold nanoparticles after 1 h of reaction time was found to be 6.6 nm with a standard deviation of 1.4 nm as observed by TEM measurements (Supporting Information Figure S1).

(d) A 12.2 nm Glucose-Reduced Gold Seed. These nanoparticle seeds were synthesized by a slight modification to the method previously demonstrated by Sastry and co-workers.[30,31] Typically, 18 mL of an aqueous solution of 2.5×10^{-4} M $HAuCl_4$ was prepared in a conical flask. To this solution was added 2 mL of 1 M D-glucose. The solution was heated to 60 °C, 40 μL of 1 M NaOH was added, and the resulting solution was subsequently stirred rapidly for 10 s. The color of the solution immediately changed to ruby red, indicating the formation of gold nanoparticles. The size of these particles as observed by TEM measurements was 12.2 ± 3.5 nm (Supporting Information Figure S2). The particles are believed to be stabilized by a monolayer of gluconic acid on the surface and thus are negatively charged.[30,31] The seed solution was cooled to room temperature and used directly for all further experiments.

(e) An 18 nm Citrate-Stabilized Gold Seed. The synthesis of these nanoparticle seeds was adapted according to the Frens method.[32] Specifically, 100 mL of an aqueous solution of 2.5×10^{-4} M $HAuCl_4$ was heated to boiling. To this was added 10 mL of an aqueous solution of 1% sodium citrate, and boiling was continued. The color of the solution first turned purple and on further boiling changed to ruby red, indicating the formation of gold nanoparticles. This method produces gold nanoparticles of the size 18 ± 3 nm as has been reported previously.[32] The seed solution was cooled and used directly for all further experiments.

Positively Charged (CTAB-Capped) Nanoparticle Seeds. All positively charged nanoparticle seeds were synthesized by the method of Jana et al.[33] These seeds could be used immediately after the synthesis and were stable for more than a month due to the presence of a bilayer of CTAB acting as stabilizer.[33] According to preliminary ζ potential measurements provided by Brookhaven Instruments, these CTAB-coated gold nanoparticles are positively charged. Typically this seeding growth method involves first the synthesis of a 3.5 nm citrate-stabilized gold seed solution (as detailed previously). Next, a growth solution was prepared wherein 100 mL of an aqueous solution of 2.5×10^{-4} M $HAuCl_4$ was taken in a conical flask. To this was added 3 g of solid CTAB (0.08 M final CTAB concentration), and the resulting solution was heated with

(24) Nikoobakht, B.; El-Sayed, M. A. *Langmuir* **2001**, *17*, 6368.
(25) Johnson, C. J.; Dujardin, E.; Davis, S. A.; Murphy, C. J.; Mann, S. *J. Mater. Chem.* **2002**, *12*, 1765.
(26) Gai, P. L.; Harmer, M. A. *Nano Lett.* **2002**, *2*, 771.
(27) Sun, Y.; Mayers, B.; Herricks, T.; Xia, Y. *Nano Lett.* **2003**, *3*, 955.
(28) Gao, J.; Bender, C. M.; Murphy, C. J. *Langmuir* **2003**, *19*, 9065.
(29) Patil, V.; Malvankar, R. B.; Sastry, M. *Langmuir* **1999**, *15*, 8197.
(30) Gole, A.; Kumar, A.; Phadtare, S.; Mandale, A. B.; Sastry, M. *PhysChemComm* **2001**, *19*, 1.
(31) Mayya, K. M.; Jain, N.; Gole, A.; Langevin, D.; Sastry, M. *J. Colloid Interface Sci.* **2004**, *270*, 133.
(32) Frens, G. *Nature* **1973**, *241*, 20.
(33) Jana, N. R.; Gearheart, L.; Murphy, C. J. *Langmuir* **2001**, *17*, 6782.

stirring. The solution was cooled to room temperature and used as a stock solution.

(a) A 5.6 nm Seed. A 7.5 mL aliquot of the growth solution was mixed with 50 μL of freshly prepared 0.1 M ascorbic acid solution. Next, 2.5 mL of the 3.5 nm seed solution was added with stirring. The color immediately turned ruby red, indicating the formation of gold nanoparticles. Stirring was continued for a further 10 min for complete reduction of the gold salt. Particles prepared by this way were spherical with a diameter of 5.6 $\pm$ 0.6 nm.

(b) An 8 nm Seed. A 9 mL sample of the growth solution and 50 μL of 0.1 M ascorbic acid solution were mixed, and 1.0 mL of the 3.5 nm seed solution was added with vigorous stirring. Stirring was continued for an additional 10 min. The final color of the solution was dark red, and the particles prepared by this method were 8.0 $\pm$ 0.8 nm. The particles prepared here were used as seeds for preparing 16 nm particles (see below).

(c) A 16 nm Seed. A 9 mL sample of the growth solution was mixed with 50 μL of 0.1 M ascorbic acid solution, and 1.0 mL of the 8.0 nm seed solution (as synthesized above) was added with vigorous stirring. After 10 min of stirring, the purple-colored solution showed a particle size of 16 $\pm$ 2.5 nm according to TEM.[33]

Gold seeds were also synthesized by the method described by Nikoobakht and El-Sayed.[23] Specifically, to a 10 mL 0.1 M aqueous solution of CTAB was added 250 μL of 0.01 M $HAuCl_4$. To the stirred solution was added 0.60 mL of 0.01 M sodium borohydride, which resulted in the formation of a brown-yellow solution. Vigorous stirring of the seed solution, which was kept at 25 °C, was continued for 2 min. Note that the concentration of borohydride in this case is 10 times less than that used by us for the synthesis of gold seeds. This seed solution was further used for the synthesis of gold nanorods after 30 min of its synthesis. The size of these seed particles was less than 4 nm.[23]

Synthesis of Gold Nanorods. Gold nanorods were synthesized by the three-step seeding protocol as described previously.[18] Specifically, two 20 mL conical flasks and one 100 mL conical flask (labeled A, B, and C, respectively) were taken. To these flasks were added 9 mL (in flasks A and B) and 45 mL (in flask C) of growth solution containing a mixture of 2.5×10^{-4} M $HAuCl_4$ and 0.1 M CTAB solutions. To these solutions were added 50 μL (flasks A and B) and 250 μL (flask C) of 0.1 M freshly prepared ascorbic acid, and the resulting solutions were stirred gently. The orange color of the gold salt in the CTAB solution disappeared when ascorbic acid was added. We have attributed this color change to the reduction of Au^{3+} to Au^{+}. However, the reduction of Au^{+} to Au^{0} does not occur, and we do not observe the gold plasmon band indicative of Au^{0} nanoparticles even after 24 h. This indicates that ascorbic acid is too weak to reduce Au^{+} under our experimental conditions. However, further reduction of Au^{+} to Au^{0} occurs when 1.0 mL of the seed solution is mixed with sample A (step 1). This is evidenced by a rapid development of red color to the solution in sample A, which earlier was colorless, thus indicating the formation of gold nanoparticles. After 15 s, 1.0 mL of sample A was mixed with sample B (step 2). This leads to a color change in sample B, indicating the generation of gold nanoparticles. The reduction in this case is slower compared to that in step 1. A 5.0 mL portion of sample B was further added to sample C after 30 s (step 3). The color of this solution slowly changed to purple. In all cases, each flask was gently stirred to homogenize the solutions. The solution in flask C was kept at 25 °C for a period of 16 h.

After the solution was stored for 16 h, purification was necessary to obtain gold nanorods. All the top red-brown solution (which contains mostly spheres) was slowly removed by suction. A faint brown tinge can be observed at the bottom of the flask. A 5.0 mL sample of deionized water was flushed into the beaker, and the contents were agitated for some time. A brown color developed in the deionized water and intensified upon repeated agitation. This solution contains a high percentage of gold nanorods, though other shapes (triangles, hexagons, and small rods) are also present. It was difficult to further purify the rods of the different shapes, and hence, we have included them in our analysis of the rods. The excess CTAB was removed by centrifugation twice (at 7000 rpm) and washing with deionized water.

Different sets of experiments were performed wherein the nature and the size of the seed solution were varied. Simple calculations suggest that, as the size of the seed increases, the total number of gold atoms required per seed particle increases. For instance, a single 4 nm seed particle has ca. 1980 atoms of gold, and a single 8 nm seed particle contains ca. 15854 gold atoms (considering an fcc crystal lattice for gold with cube dimensions of 4.08 Å per side, with 4 gold atoms per unit cell). For the same concentration of initial gold atoms in both the cases (2.5×10^{-4} M), this indicates a decrease in the total number of seed particles per unit volume. Hence, to maintain the same number of seed particles in all the cases, one has to increase the volume of the seed solution as the seed size increases. Simple calculation suggests that, if 1 mL of the 4 nm seed solution is normally used for the synthesis of rods by our protocol, then as the size of the seed increases to ca. 8 nm, we would require 8.4 mL of the seed solution to maintain the same number of seeds. To maintain the volume of the seed/gold salt solution, we have concentrated (by centrifugation) the seed solution to 1 mL. We use this solution (8.4 mL concentrated to 1 mL) to further synthesize gold nanorods by our protocol. Similar calculations were performed for all the seed particles and were used appropriately. No aggregation of particles upon concentration was observed as determined by UV−vis spectroscopy. Furthermore, the gold nanorods were synthesized 3−4 times by the method detailed above and subsequently analyzed by TEM measurements (see below). This was done to confirm reproducibility of the data.

Transmission Electron Microscopy. TEM measurements were performed on a Hitachi H-8000 TEM instrument operating at an accelerating voltage of 200 kV. A 3 μL drop of the gold nanorod solution (centrifuged and resuspended in deionized water) was dried on carbon-coated copper grids for 1 h.

As mentioned above, each set of gold nanorods were synthesized thrice and individually studied by TEM measurements. TEM micrographs of at least three different regions of the grid were recorded, and for each set of nanorods ca. 150−200 particles were counted and measured to determine the nanorod dimensions and particle distributions.

UV−Vis/Near-IR Measurements. The centrifuged gold nanorod pellet was resuspended in deuterium oxide (D_2O) for UV−vis/near-IR measurements which were performed on a Varian model Cary 500 Scan UV−vis/near-IR spectrophotometer. Care was taken to rinse the quartz cuvette (in deionized water) and dry it in a jet of flowing nitrogen prior to each measurement.

Fourier Transform Infrared Spectroscopy Measurements. The gold nanorod samples (after removal of uncoordinated CTAB molecules by centrifugation and resuspension) were drop dried on 4 cm^2 Si(111) substrates. The samples were analyzed on a Nexus Thermo-Nicolet 470 series FTIR instrument coupled with a Thermo-Nicolet Continumm FTIR microscope in the reflection mode. A total of 128 scans of each sample were recorded at a resolution of 4 cm^{-1}.

Results and Discussion

As mentioned in the Experimental Section, gold nanorods were synthesized by the seed-mediated surfactant-assisted (CTAB) three-step protocol. This is schematically represented in Scheme 1. As can be seen, introduction of a seed leads to generation of nonspherical gold nanoparticles. We have previously[25] suggested that the binding of CTAB to specific crystal faces leads to anisotropic (1-D) growth of the nanocrystals. Control of the nanorod aspect ratio was only performed in the growth steps using the same 3.5 nm citrate-capped seed

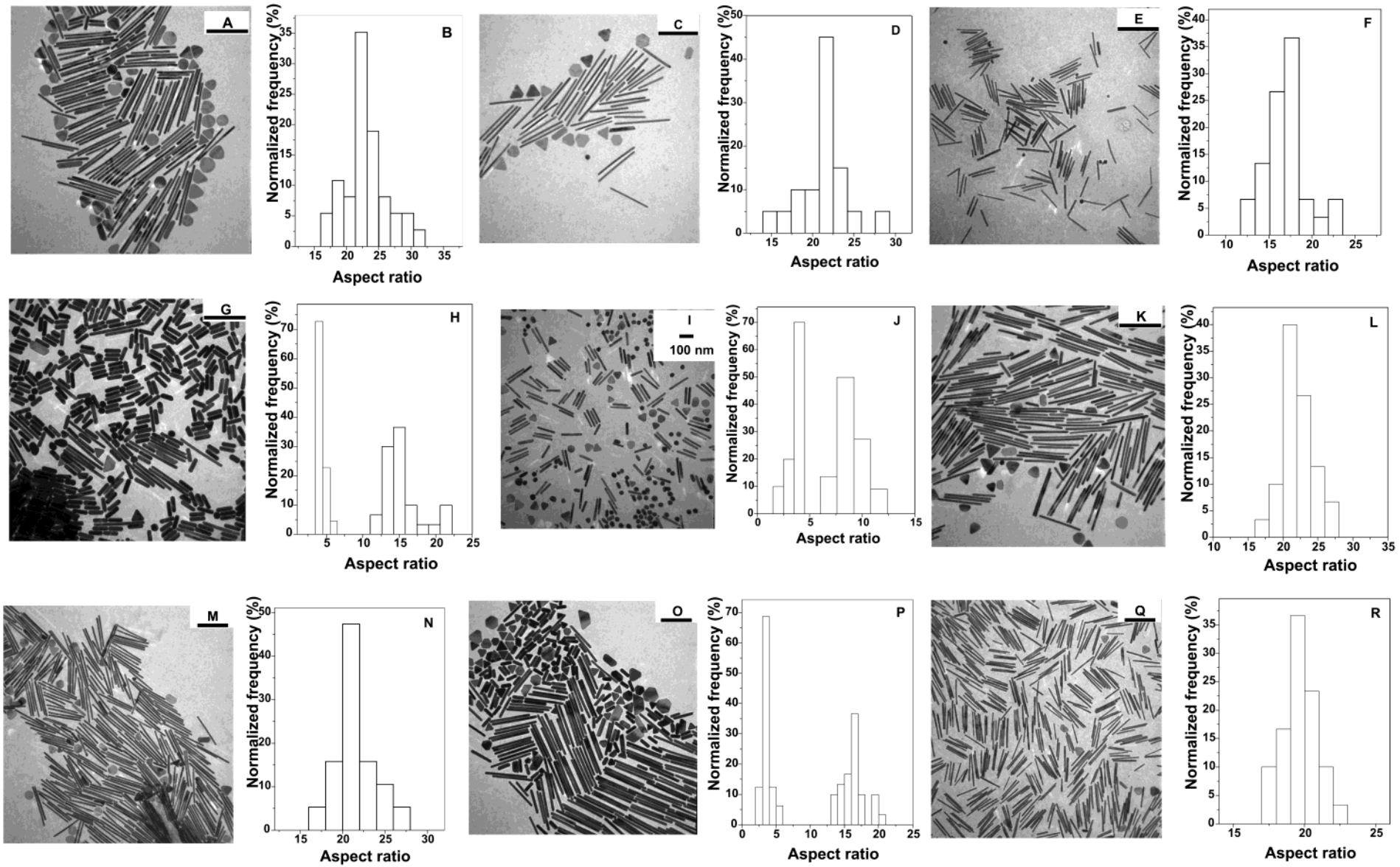

Figure 1. (A−R) TEM micrographs of gold nanorods synthesized from different seeds and their respective particle size histograms. The seeds used were (A, B) a 3.5 nm citrate-stabilized seed, (C, D) a 3.5 nm borohydride-reduced uncapped seed, (E, F) a 4-MBA-capped 6.6 nm seed, (G, H) a 12.2 nm glucose-reduced gold seed, (I, J) a citrate-stabilized 18 nm seed, (K, L) a CTAB-stabilized 5.6 nm seed, (M, N) a CTAB-stabilized 8 nm seed, (O, P) a CTAB-stabilized 16 nm seed, and (Q, R) a CTAB-stabilized seed prepared by the Nikoobakht and El-Sayed method.[23] The scale bars in each micrograph measure 500 nm (except micrograph I, where the scale bar measures 100 nm).

Scheme 1. General Methodology for the Generation of Gold Nanorods

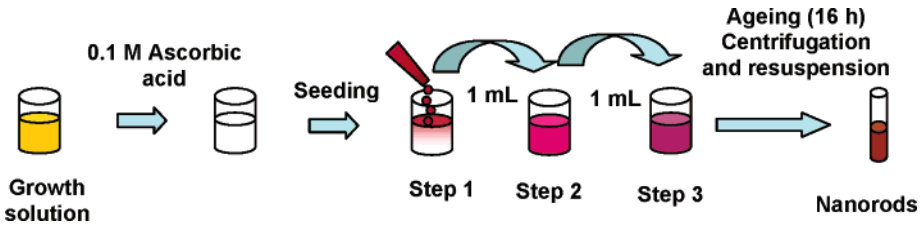

Table 1. Average Lengths, Widths, and Aspect Ratios of the Long Gold Nanorods Synthesized from Different Seeds

negatively charged seeds used for gold nanorod synthesis				positively charged (CTAB) capped seeds used for gold nanorod synthesis			
seed size (nm)	nanorod length (nm)	nanorod width (nm)	aspect ratio	seed size (nm)	nanorod length (nm)	nanorod width (nm)	aspect ratio
3.5 (citrate)	621 ± 70	27.5 ± 2.0	22.9 ± 2.5	<4	468 ± 34	24.1 ± 2.0	19.4 ± 1.4
3.5 (uncapped)	663 ± 62	31 ± 3.0	21.1 ± 1.9	5.6	564 ± 63	24.8 ± 2.0	22.6 ± 2.4
6.6 (4-MBA)	340 ± 38	20.5 ± 3.0	16.5 ± 1.8	8	500 ± 52	23.4 ± 2.0	21.2 ± 2.2
12.2 (glucose)	561 ± 110	36.2 ± 2.0	15.4 ± 3.0	16	667 ± 56	40.9 ± 2.0	16.6 ± 1.3
18 (citrate)	150 ± 20	16.7 ± 2.0	8.9 ± 1.1				

in our previous studies.[25] Here we examine the importance of the seed in the synthesis of gold nanorods.

Direct visualization of the seed effects in gold nanorod synthesis can be seen by TEM measurements. Figure 1 shows some of these images and their respective particle size histograms. The images and corresponding histograms have been displayed for decreasing aspect ratios (Figure 1A−J for negatively charged seeds and Figure 1K−P for positively charged seeds). For differently sized seeds, care was taken to maintain the same concentration for all the seed particles as explained in the Experimental Section. It was observed that, for negatively charged seeds, the nanorod aspect ratios varied as ca. 22.9 ± 2.5 for the 3.5 nm citrate-stabilized seeds (Figure 1A,B), 21.1 ± 1.9 for the 3.5 nm uncapped seeds (Figure 1C,D), 16.5 ± 1.8 for the 6.6 nm 4-MBA-capped seeds (Figure 1E,F), 15.4 ± 3 for the 12.2 nm glucose-reduced seeds (Figure 1G,H), and 8.9 ± 1.1 for the citrate-stabilized (Frens method[32]) 18 nm seeds (Figure 1I,J). For positively charged seeds (CTAB-stabilized), the nanorod aspect ratios fall in the range 22.6 ± 2.4 for the 5.6 nm seed (Figure 1K,L), 21.2 ± 2.2 for the 8 nm seed (Figure 1M,N), and 16.6 ± 1.3 for the 16 nm seed (Figure 1O,P). In all the cases, along with a large concentration of long rods, a small number of different shapes such as triangles, hexagons, and small rods are observed. The proportion of high-aspect-ratio rods decreases with an increase in the seed size used for nanorod synthesis. Overall, there is a general trend of a decrease in the aspect ratio of the gold nanorods with an increase in the seed size (see below).

The CTAB-stabilized seeds synthesized by the Nikoobakht and El-Sayed method[23] (seed size <4 nm) have also been used for the synthesis of gold nanorods by the three-step protocol, and the TEM image and its particle size histogram are shown as Figure 1Q,R. The gold nanorod aspect ratio is 19.4 ± 1.4 in this case, and is lower compared to the aspect ratio of gold nanorods synthesized by the CTAB-capped 5.6 and 8 nm seeds. As mentioned earlier, the general trend observed in all the cases is a decrease in the aspect ratio of the gold nanorods as a function of an increase in the seed size (Figures 1A−P and 2; see below). This clearly indicates that these seeds (Nikoobakht and El-Sayed method[23]) do not follow the general trend observed. This might be due to the uncertainty in the exact size of the seed; due to the difficulty of removing excess CTAB molecules (by centrifugation) accurate TEM analysis of the seed size was problematic. Hence, we have assumed the size of the particles to be less than 4 nm as mentioned by Nikoobakht and El-Sayed.[23]

Figure 2 shows the variation of aspect ratios of the gold nanorods synthesized using different negatively charged seeds (circles, Figure 2A) and positively charged seeds (circles, Figure 2B) wherein the concentration of the seeds is the same. The solid lines in both the cases are linear least-squares fits to the data. The vertical lines to the data points are error bars in both the cases (Figure 2). It can be seen that for negatively charged

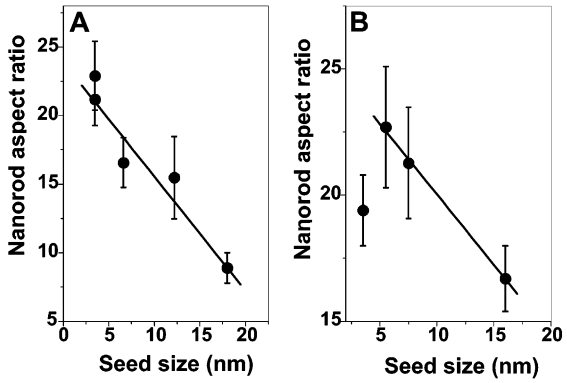

Figure 2. (A) Variation of the aspect ratio of gold nanorods as a function of the size of the negatively charged seeds used for the synthesis of nanorods. The solid line is a linear fit to the data. The vertical lines to the data points are the error bars. (B) Variation of aspect ratio of gold nanorods as a function of the size of the positively charged seeds used for the synthesis of nanorods. The solid line is a linear fit to the data. The vertical lines to the data points are the error bars.

3.5 nm seeds (citrate-capped and uncapped), the aspect ratio of gold nanorods synthesized is similar and within the error limits. Furthermore, the overall trend for both positively charged and negatively charged seeds is that, as the size of the seed increases, the aspect ratio of the synthesized nanorods decreases. The variation of the aspect ratios as a function of seed size is more pronounced when negatively charged seeds are used for nanorod synthesis (aspect ratio varies from ca. 23 to ca.

Table 2. Average Number of Differently Shaped Particles (Triangular, Hexagonal, Spherical, and Rod) Synthesized (after Purification) from Different Seeds

seed size (nm)	big rod concn (%)	small rod concn (%)	triangle concn (%)	hexagon concn (%)	sphere concn (%)
3.5 (citrate)	77 ± 3	10 ± 4	8 ± 2	3 ± 1	0
3.5 (uncapped)	74 ± 2	10 ± 4	13 ± 1	4 ± 2	0
6.6 (4-MBA)	86 ± 3	9 ± 1	2	0	5 ± 2
12.2 (glucose)	17 ± 1	79 ± 3	1	2	1
18 (citrate)	43 ± 2	12 ± 2	10 ± 3	2	32 ± 4
5.6 (CTAB)	82 ± 2	10 ± 2	5 ± 1	2 ± 1	0
8 (CTAB)	80 ± 4	8 ± 1	3 ± 2	3 ± 1	0
16 (CTAB)	55 ± 4	27 ± 2	14 ± 3	3 ± 1	1
<4 (CTAB)	84 ± 1	11 ± 2	3 ± 1	0	0

9) compared to positively charged seeds (aspect ratio varies from ca. 22 to ca. 16). The different parameters such as length, width, and aspect ratio of the gold nanorods synthesized using different seeds are displayed in Table 1. It can be seen from the table that variation in the length and the width also follows a trend as a function of seed size for negatively charged seeds. As the size of the seed increases, the final nanorods are generally reduced in length and in width. For positively charged seeds, no general trend in nanorod length and width was observed. The presence of triangular, hexagonal, and spherical particles along with short and long rods can also be clearly seen in the TEM images of Figure 1. The shape distribution is displayed in Table 2. It is interesting to note that big seed particles (≥12 nm) produce a significant amount of small rods and other secondary shapes. Furthermore, the glucose-reduced gold seeds (12.2 nm) produce a large number of smaller rods compared to longer ones. A simple diagram displaying the growth of gold nanorods as a function of the size of the seed is given in Scheme 2.

Scheme 2. Different Stages of Growth of Gold Nanorods for Small (5.5 nm) and Big (8 nm) Seed Particles

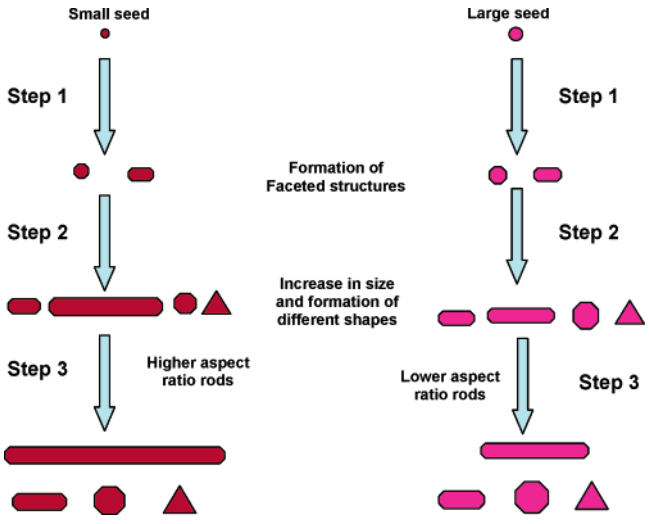

UV−vis spectroscopy was performed on the gold nanorod samples, and a number of bands were observed. The band of our interest around 1400 nm in all the cases is due to the longitudinal plasmon resonance of long gold nanorods and has been detailed in the inset of Figure

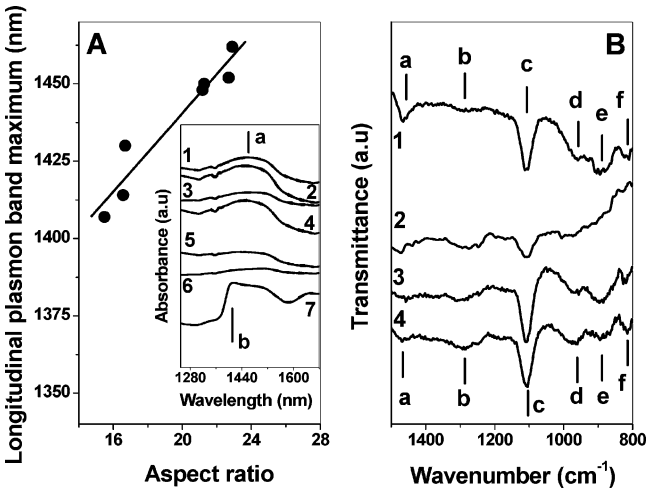

Figure 3. (A) Variation of the position of the longitudinal plasmon maximum bands for gold nanorods as a function their respective aspect ratios. The solid line is the linear least-squares fit to the data. The inset shows the UV−vis data for the longitudinal plasmon resonance for the different gold nanorods synthesized using different seeds: curve 1, a 3.5 nm citrate-stabilized seed; curve 2, a CTAB-stabilized 5.6 nm seed; curve 3, a CTAB-stabilized 7.5 nm seed; curve 4, a 3.5 nm borohydride-reduced uncapped seed; curve 5, a CTAB-stabilized 16 nm seed; curve 6, a 4-MBA-capped 6.6 nm seed; curve 7, a 12.2 nm glucose-reduced gold seed. (B) FTIR spectra in the 1500−800 cm^{-1} region of drop-dried gold nanorod solutions prepared by different seeds: curve 1, a 3.5 nm citrate-stabilized seed; curve 2, a 3.5 nm borohydride-reduced seed; curve 3, a 7.5 nm CTAB-stabilized seed; curve 4, a 16 nm CTAB-stabilized seed. Assignments: a, 1465 cm^{-1}; b, 1285 cm^{-1}; c, 1110 cm^{-1}; d, 960 cm^{-1}; e, 890 cm^{-1}; f, 815 cm^{-1}.

3A. The presence of this band indicates the big gold nanorods as seen by TEM measurements (Figure 1). It has been established by Nikoobakht and El-Sayed[23] that the position of this band is sensitive to the aspect ratio of the gold nanorods. There is clearly a red shift in the position of this band as the aspect ratio of the gold nanorod increases. This shift has been marked by two solid lines: point a at 1460 nm for gold nanorods of aspect ratio 23 and point b at ca. 1407 nm for gold nanorods of aspect ratio 15. The main part of Figure 3A shows the variation of the longitudinal plasmon resonance maximum (at ca. 1400 nm) as a function of the aspect ratio of the gold nanorods. The solid line is a linear least-squares fit to the data. Such a trend has been observed previously for shorter gold nanorods.[23] The other bands at ca. 500, around 800, and around 1050 nm, the former being the transverse plasmon band and the latter two being due to triangular and hexagonal particles, can be seen in the UV−vis/near-IR spectra displayed as Supporting Information Figure S3. Such plasmon bands have been previously observed for triangular and hexagonal particles.[34,35]

To check the presence of a CTAB bilayer on the surface of the gold nanorods synthesized, and to understand its nature of interaction with the gold nanorods, we have performed FTIR measurements. The purified samples were drop dried on Si(111) substrates, and

(34) Hao, E.; Bailey, R. C.; Schatz, G. C.; Hupp, J. T.; Li, S. *Nano Lett.* **2004**, *4*, 327.
(35) Malikova, N.; Pastoriza-Santos, I.; Schierhorn, M.; Kotov, N. A.; Liz-Marzan, L. M. *Langmuir* **2002**, *18*, 3694.

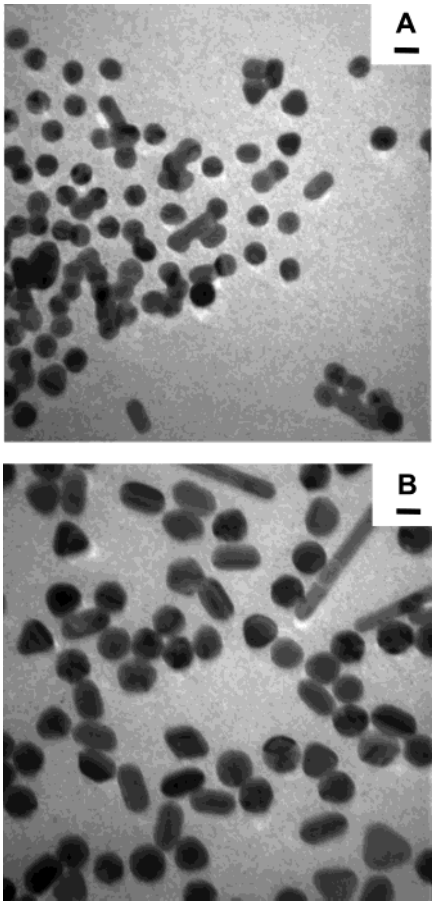

Figure 4. TEM micrographs of the (A) first and (B) second growth stages of the gold nanorods wherein a 5.6 nm CTAB stabilized gold seed has been used for nanorod synthesis. Scale bars 20 nm.

FTIR spectra were recorded on different regions of the dried sample. Si substrates were chosen for FTIR measurements as they do not show any features in the infrared window of our interest (400−4000 cm^{-1}). Methylene symmetric and antisymmetric vibrations were observed for all the samples recorded, indicating the presence of CTAB in the sample. The 1500−800 cm^{-1} region was used to analyze the nature of interaction between the CTAB molecules and the gold nanorods as shown in Figure 3B. For simplicity we have displayed four FTIR spectra of the different nanorods synthesized by negatively or positively charged seeds. Curves 1−4 indicate the nanorod samples, where the seeds used are (curve 1) a citrate-stabilized 3.5 nm seed, (curve 2) a 3.5 nm uncapped gold seed, and (curves 3 and 4) CTAB-stabilized 8 and 16 nm seeds, respectively. A number of spectral features can be clearly seen in all the cases. A feature at ca. 1465 cm^{-1} arises due to the CH_2 scissoring modes of vibration[23] (feature a, Figure 4). The band at 1280 cm^{-1} arises due to the C−N stretch vibrations of the CTAB molecule (feature b, Figure 4). The absence of the bands at 937 and 912 cm^{-1} and furthermore the presence of bands at 1107, 960, 890, and 817 cm^{-1} (features c, d, e, and f, Figure 4) clearly indicate the binding of CTAB molecules to the gold nanorods via the CTA^+−Au linkage.[23] The presence of these bands compares well with that observed by Nikoobakht and El-Sayed[23] and clearly indicates the presence of a bilayer of CTAB capping the gold nanorods.

To summarize, the gold nanorod aspect ratio depends linearly on the size of the seed used for its synthesis. This is true for both positively and negatively charged seeds (Figure 2). Furthermore, larger seeds (>8 nm) produce a significant amount of short nanorods along with longer nanorods (Figure 1, micrographs G, I, and O and their corresponding histograms H, J, and P, respectively). The capping agents on the seed particles also play a role in the nanorod synthesis. Specifically, the variation in the aspect ratios of gold nanorods synthesized by positively charged seeds is less compared to that of the negatively charged seeds. Furthermore, for negatively charged seeds some interesting data are observed. The 3.5 nm gold seeds either capped (by citrate) or uncapped produce gold nanorods that have similar aspect ratios (within the error bars) as seen in Figure 2A. Glucose-reduced gold seeds used for the synthesis of nanorods produce a larger number of shorter nanorods compared to longer nanorods (Table 2). All these variations can be explained by analyzing the process of formation of the nanorods. As explained earlier, nanorod synthesis can take place due to the preferential binding of CTAB to specific crystal faces during the nanocrystal growth.[25] We believe that rearrangement or replacement of any prebound molecule on the seed by the abundantly available CTAB molecules in the growth solution is a first step in this process. As CTAB-capped (positively charged) seeds can possibly mix well with the growth solution due to the similar chemical functionality, the variation in the nanorod aspect ratio formed is less pronounced. The covalently bound 4-MBA molecule might be difficult to detach and results in unusually thin and short nanorods with a still reasonably high aspect ratio. The interactions between the different surface groups on the seeds with the growth solution are not well understood at this stage.

Shape and Size Evolution of Gold Nanocrystals. Attempts have been made by a number of researchers to understand the process of nucleation and growth for nanocrystals.[23,25−27] As far as nucleation and growth is concerned, we have previously studied in detail such a process involving synthesis of differently sized gold nanoparticles.[33,36] As mentioned earlier, when seed particles are introduced in a solution containing Au^+ ions (Au^+ is first formed by reduction of Au^{3+} to Au^+ by the mild reducing agent ascorbic acid), they act as nucleation centers catalyzing the reduction of Au^+ to Au^0 on their surfaces. Thus, under normal conditions, introduction of a seed produces particles which are bigger than the seed. At some stage, facets are developed, and at this point some of these particles could be directed to grow into nanorods. Petroski et al.[37] have studied the shape distribution of platinum nanoparticles at different stages of their growth as a function of time. They provide two reasonable explanations for the formation and evolution of tetrahedral, truncated octahedral, and cubic-shaped particles: (i) the growth rates vary at different planes of the particles and (ii) particle growth competes with the capping action of stabilizers. A similar scenario might be operative in our case wherein introduction of a seed leads to rapid reduction

(36) Jana, N. R.; Gearheart, L.; Murphy, C. J. *Chem. Mater.* **2001**, *13*, 2313.
(37) Petroski, J. M.; Wang, Z. L.; Green, T. C.; El-Sayed, M. A. *J. Phys. Chem. B* **1998**, *102*, 3316.

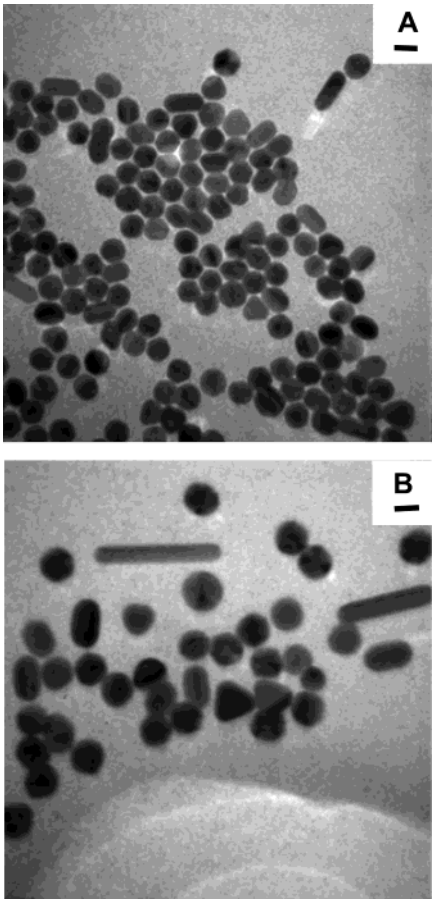

Figure 5. TEM micrographs of the (A) first and (B) second growth stages of the gold nanorods wherein an 8 nm CTAB-stabilized gold seed has been used for nanorod synthesis. Scale bars 20 nm.

of gold salt on the seed surface. The competitive and preferential binding of CTAB molecules on the (100) surface possibly leads to the generation of faceted spheres which evolve to form rods. This is also supported by our previous HR-TEM studies wherein we have demonstrated that in fcc metallic structures symmetry breaking by twinning introduces anisotropy in the shape of the nanocrystal.[25] This coupled with the preferential binding of CTAB to the (100) crystal face arrests growth in this direction, and leads to the formation of nanorods.[25]

It is reasonable to believe that the shape and size of the nanorods formed would depend on the history of the different stages involved in nanorod formation. To investigate these effects, we performed TEM measurements on the different stages of nanocrystal growth in our three-step protocol. Figures 4 and 5 show the TEM micrographs of the first and second stages of the nanorod synthesis wherein CTAB-capped 5.6 and 8 nm seeds were used. Faceted nanocrystallites can be clearly seen in both the steps (Figures 4 and 5). The size of the faceted nanospheres synthesized for steps 1 and 2 where a 5.6 nm seed was used are 19.9 ± 1.7 nm (Figure 4A) and 31.2 ± 2.2 nm (Figure 4B), respectively. Similarly for an 8 nm seed used for the synthesis of nanorods, the two stages produce nanospheres of sizes 22.4 ± 1.0 nm (Figure 5A, stage 1) and 32.2 ± 1.8 nm (Figure 5B, stage 2). The size of the nanospheres formed in both the cases is greater than that of the injected seed, suggesting growth on the preformed seeds (as opposed to new seeds being formed). Some nanorods can be clearly seen in both the cases, and their dimensions increase with each seeding step. The nanorods synthesized in step 2 in both the cases have aspect ratios of ca. 8.8 (5.6 nm seed used) and ca. 7.1 (8 nm seed used). It can be seen that the difference in the aspect ratios of the nanorods synthesized by the two differently sized seeds is evident even at these stages of nanocrystal growth. In the third and final step of crystal growth, one can thus see the formation of larger nanorods (Figure 1, micrographs K and M, respectively). Such increased growth of the nanospheres and formation of nanorods in different stages was previously observed by us for the 4 nm size citrate-stabilized gold seeds used for nanorod synthesis, wherein the mean diameter of the particles for the two steps increased from ca. 9.6 to 17.4 nm.[25] Comparison of these results clearly supports that the size and shape and its subsequent evolution to form gold nanorods are all controlled by the initial gold nanoparticle seed size.

Conclusion. We have shown that gold nanorods can be synthesized by using a variety of different seeds with different sizes and surface functionalities. The aspect ratio of the nanorods, to a large extent, increases as the seed size decreases. The changes in the dimensions of the nanorods as a function of seed size are more pronounced in negatively charged seeds compared to positively charged seeds. Our previous studies indicate twinning and preferential binding of CTAB molecules on the (100) crystal face, as a mechanism for the nanorod synthesis and growth. We have studied the seed size dependence on the shape and size of the nanorods synthesized by studying the preceding stages of the nanorod formation. We believe that these initial stages help determine the final nanorod size and shape formation.

Acknowledgment. We thank M. L. Myrick and D. Perkins for assistance with the FTIR instrument.

Supporting Information Available: Transmission electron micrographs of selected seed nanoparticles and UV−vis spectra of the final gold nanorods (PDF). This material is available free of charge via the Internet at http://pubs.acs.org.

CM0492336